Spatiotemporal dynamics in a dispersively coupled chain of nonlinear oscillators

David K. Umberger,* Celso Grebogi, Edward Ott,† and Bedros Afeyan‡
Laboratory for Plasma Research, University of Maryland, College Park, Maryland 20742
(Received 17 October 1988)

A one-dimensional chain of forced nonlinear oscillators is investigated. This model exhibits typical behavior in periodically forced, spatially extended, nonlinear systems. At low driving amplitudes characteristic domainlike structure appears accompanied by simple asymptotic time dependence. Before reaching its final state, however, the chain behaves chaotically. The chaotic transients appear as intermittent bursts mainly concentrated at the domain walls. At higher driving, the chaotic transient becomes longer and longer until the time dependence apparently corresponds to sustained chaos with the chain state characterized by the absence of domainlike spatial structure.

I. INTRODUCTION

In the past, most of the work on chaotic dynamics has been concentrated on the temporal behavior of low-dimensional systems. Many physical systems of interest, however, as fluid flows, require the study of very high-dimensional systems which have intricate spatial and temporal evolution properties. Models which might reveal, therefore, some of the fundamental properties of spatially extended nonlinear systems are of great interest. One such model is proposed and studied in this work.

For low-dimensional systems, the Poincaré surface of section technique transforms continuous time systems (flows) into discrete time systems (maps). Furthermore, simple maps not necessarily derived from Poincaré surfaces of section (e.g., the quadratic map, the Hénon map, etc.) have served as useful models displaying typical temporal behavior of low-dimensional dynamical systems. This has motivated the suggestion that spatiotemporal phenomena, characteristic of continuous space-time systems (such as described by partial differential equations) might be modeled by systems that are discrete in both space and time.[1,2] Work along these lines has revealed that a class of coupled map lattices can exhibit spatial domain like structures (kink-antikink patterns, for example). Furthermore, it has been shown that these systems can exhibit highly nontrivial behavior such as spatial intermittency, period doubling of kink-antikink patterns, the coexistence of laminar and chaotic regions, and so forth.

It is, however, an open question whether phenomena in coupled map lattice systems are really indicative of typical phenomena in systems that are continuous in time and space. An intermediate approach, which might be used to bridge the gap between continuous space-time systems and discrete time systems, is a system that is continuous in time and discrete in space. The systems considered here consist of simple second-order ordinary differential equations defined on a one-dimensional lattice of oscillators with nearest-neighbor coupling. A mechanical realization of the system we consider is illustrated in Fig. 1. In the uncoupled limit the basic ordinary differential equation (ODE) describing the dynamics of each oscillator is chosen to be the forced Duffing equation.[3] This equation is known to display a rich variety of dynamical behavior: from periodic to chaotic solutions, multiple attractors, and fractal basin boundaries.

For the specific parameter values we use to investigate our coupled ODE lattice system, we observe two regimes, one at relatively low forcing and one with a somewhat higher forcing. In the first case we observe the formation of spatial domains where groups of neighboring lattice points are in similar states. Furthermore, these low forcing cases evolve to a state which is periodic with the same period as the driving, i.e., a *fixed point* of the time one stroboscopic map (Poincaré). Even though the final state is a simple one,the transient dynamics[4] through which the system passes is rich in structure. In particular, we observe *extremely* intermittent behavior wherein the time evolution of a given oscillator alternates irregularly between slowly evolving periods and periods of rapid chaotic oscillation. These oscillation patterns propagate along the chain. These spatially structured chaotic transients appear to be very typical in this system. In the strongly forced case, the system seems to evolve as sustained chaotic final state. Here, the spatial patterns are irregular with no apparent domain structure. In common with the lower forcing case, the tendency for extremely intermittent temporal behavior persists, but now it is sustained rather than transient.

In Sec. II we introduce and discuss the specific system studied. In Sec. III we present numerical results and their interpretations. Section IV presents conclusions.

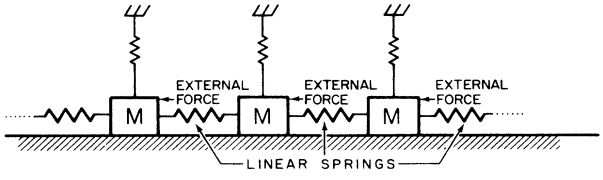

FIG. 1. Illustration of the unforced coupled ODE lattice chain.

II. COUPLED ORDINARY DIFFERENTIAL EQUATION LATTICE SYSTEM

The chain of nonlinear oscillators whose behavior we investigate is a collection of N forced Duffing oscillators coupled via a linear dispersive term whose equations of motion are

$$\ddot{x}_i(t)=-\gamma\dot{x}_i(t)+\frac{\sigma}{2}x_i(t)[1-x_i^2(t)] +f\cos(\omega_D t)+\varepsilon D_2[x_i(t)]\ , \quad (1)$$

where $i=1,\ldots,N$. Dots denote differentiating with respect to the time t, and D_2 is the second spatial differencing operator

$$D_2[x_i]\equiv x_{i+1}-2x_i+x_{i-1}\ . \quad (2)$$

The variable $x_i(t)$ is the displacement at time t of the ith oscillator from its point of unstable equilibrium in the absence of damping, driving, and coupling. The parameters γ, σ, f, ω_D, and ε are, respectively, the damping strength, the strength of the restoring force, the amplitude and frequency of the external driving, and the coupling strength. We use periodic boundary conditions $x_0=x_N, x_1=x_{N+1}$.

Taking a Poincaré surface of section of the system, Eq. (1) results in a coupled map lattice. The section is obtained by examining the system's state after each driving period $\tau=2\pi/\omega_D$. Letting $v_i(t)\equiv\dot{x}_i(t)$ denote the velocity of the ith oscillator at time t, the state of the system at time $t=n\tau$ with n an integer is given by the $2N$-tuple $\xi_n\equiv(x_1(n\tau),\ldots,x_N(n\tau),v_1(n\tau),\ldots,v_N(n\tau))$. Then, the sequence of states ξ_k, for $k=0,1,\ldots$, is generated by a deterministic, discrete-time dissipative map $\hat{T}$, which takes ξ_k into ξ_{k+1}. That is, $\xi_{k+1}=\hat{T}(\xi_k)$. The map $\hat{T}$ differs from the most commonly studied coupled map lattice systems[1,2] in three important respects. First, $\hat{T}$ is invertible and, hence, it mimics a flow. Second, it takes two variables per site to specify its state rather than one, as is the case in coupled logistic maps, for example. Third, and most important, as our system is integrated over one driving period τ, the motion of any fixed oscillator can, depending on the system parameters, be influenced by oscillators quite far away. The range of interaction depends on, among other things, the coupling strength and the damping. Hence, the map $\hat{T}$ typically exhibits long-range coupling, even though the system described by Eq. (1) has a nearest-neighbor coupling. On the other hand, except for a few notable examples, previous work on coupled map lattices were strictly limited to nearest-neighbor coupling.[2]

To show how a coupled set of ordinary differential equations can bridge the gap between coupled map lattices and partial differential equations, we seek to obtain the continuous limit of a dispersively coupled Duffing chain of oscillators. The continuum limit of Eq. (1) can be shown to be

$$\frac{\partial^2\psi}{\partial t^2}=-\gamma\frac{\partial\psi}{\partial t}+\frac{\sigma}{2}\psi(1-\psi^2)+f\cos(\omega_D t)+\varepsilon\frac{\partial^2\psi}{\partial z^2}\ . \quad (3)$$

The correspondence between Eqs. (1) and (3) is seen readily by making the heuristic substitutions $i\to z$, $x_i(t)\to\psi(z,t)$, and $D_i\to\partial^2/\partial z^2$. We expect that as N is increased in Eq. (1), its solutions approach solutions of Eq. (3) more and more closely. Linearizing Eq. (3) about the stable equilibria $\psi_0=\pm1$ and assuming the usual harmonic space-time dependence of the form $\psi\sim\exp(-i\omega t+ikz)$, yields the dispersion relation $\omega^2=\varepsilon k^2+\sigma-i\omega\gamma$. Thus $\sqrt{\varepsilon}$ is proportional to the group velocity of the wave, γ results in linear damping of the wave, while σ can be interpreted as a susceptibility of the medium. Setting $\sigma=0$ corresponds to waves propagating in vacuum, where there is no dispersion. In the material medium, σ causes the waves to be dispersive. Thus the coupled lattice ODE system (1) might be expected to model typical characteristic phenomena to be expected in forced, spatially extended nonlinear wave systems with dispersion and damping.

Returning to Eq. (1), we note that when the coupling is turned off, i.e., $\varepsilon=0$, the system becomes a collection of independent oscillators each having the equation of motion

$$\ddot{x}_i(t)=-\gamma\dot{x}_i(t)+\frac{\sigma}{2}x_i(t)[1-x_i^2(t)]+f\cos\omega_D t\ . \quad (4)$$

This is the equation of motion of a particle moving in a double-well potential when damping and driving are added. The well has points of stable equilibrium at $x_i=\pm1$ and a point of unstable equilibrium at $x_i=0$. The system equation (4) has been studied extensively,[3] and it has been shown numerically that it is capable of various types of behavior such as chaos and "final-state sensitivity."[5] The latter results from the coexistence of several attractors whose basins of attraction have fractal boundaries.[6] It is only natural to wonder, therefore, what types of behavior are possible in a lattice dynamical system whose local dynamics are so rich.

Some intuition from low-dimensional dynamics can be brought to bear on this question in the weak-coupling limit. In this limit, we expect that the motion of a single oscillator in the chain is qualitatively similar to a system obtained by adding noise to Eq. (4). For example, it is often found that attractors are stable under small noisy perturbations. Thus, if f, ω_D, σ, and γ are chosen so that Eq. (4) yields motion on some attractor, the corresponding noisy motion will occur on a slightly "fuzzed out" version of that attractor. We expect then that an oscillator of Eq. (1) also behaves in this way when the coupling is weak; the attractor of the full system will be, roughly, the direct product of N strange attractors of Eq. (4).

In cases where Eq. (4) has multiple attractors whose basins vary in size, the effect of adding noise is that of "washing out" the smaller basins of attraction; the external noise tends to "knock" an orbit originally in such a basin out into a basin of larger measure. If a smoothly varying initial condition is used in the corresponding, weakly coupled chain, different oscillators can tend to the different attractors of Eq. (4). The effect of the coupling will be to send oscillators originally intended for attractors with small basins into the attractors having the larger basins. Thus, we expect the coupling to "smooth out" the fine-scale structure of the basin of the local dy-

namics. This would imply that fine-scale structures of partial differential equation systems would be wiped out on a length scale determined by the coupling strength; the finer-scale structures of the basins would be eliminated.

Another important issue associated with the chain when the local dynamics has multiple attractors is that of domain formation. Recall that in such cases the effect of using smoothly varying initial conditions is to send different oscillators to different attractors when the coupling is small. Groups of nearby oscillators in the chain whose initial conditions lie in the same basin all tend towards the same attractor. Other adjacent groups tend towards different attractors, forming domains. Walls separating such domains are associated with oscillators whose initial conditions are close to basin boundaries.

III. NUMERICAL EXPERIMENTS

In this section we present the results of experiments performed by numerically integrating Eq. (1). The experiments examine the transient as well as the asymptotic behavior of the solutions of Eq. (1). The experiments are of two types. In the first type, the parameters of the system (ε, γ, σ, f, ω_D, and N) are fixed, and the initial condition ξ_0 is varied. The second type of experiment involves increasing the driving strength f with the remaining parameters and initial conditions held fixed. All the simulations were done with a fifth-order Runge-Kutta algorithm with variable step size[7] and chain length $N=256$.

We begin by examining the chain when the parameters γ, f, ω_D, and σ have values such that the local dynamics have several coexisting attractors. One such situation occurs when $\gamma=0.15$, $f=0.10$, $\omega_D=0.833$, and $\sigma=1$. (We fix $\sigma=1$ throughout this work.) For these parameter values, the single Duffing oscillator has[3] two periodic attractors with a fractal basin boundary separating their basins. As f is increased there is transition to chaotic motion at $f_c=0.12$. We investigate here the properties of the chain in both these regimes starting with the case where each single oscillator undergoes periodic motion. Using $\varepsilon=0$ (i.e., no coupling) and the initial condition

$$x_i(0)=a+0.45\sin\left[\frac{2\pi i}{N}\right], \tag{5a}$$

$$v_i(0)=0, \tag{5b}$$

with the offset $a=0.003$, we find that under $\hat{T}$ some of the oscillators asymptote to fixed points, while others asymptote to period-6 orbits. This is depicted in Fig. 2 where the displacements of the oscillators are plotted against lattice position for six successive iterates of **T** for $1025\le n\le 1031$. (We choose n large so that the transient has died down.) Evidently, there are four coexisting attractors, an *up* (positive displacement) fixed point, a *down* (negative displacement) fixed point, and a pair of period-6 limit cycles, one up and one down. The particular attractor that a given oscillator tends to depends on its initial condition. Since a smoothly varying (in space) initial condition was used, the lattice breaks up into domains determined by groups of nearby oscillators asymptoting to the same attractor. Experiments and simulations on coupled cells of chemical oscillators have shown rhythm splitting behavior[8-10] similar to that observed here (viz., part of the chain exhibits a fixed point state while other parts exhibit periodic time dependence).

As the coupling ε is increased the period-6 motion disappears, and the displacement as a function of lattice position smooths out. This is shown in Fig. 3 for $\varepsilon=1.0$, where the initial condition and the parameters of the local dynamics are the same as for Fig. 2. Note that, unlike Fig. 2, the state shown in Fig. 3 is a fixed point of $\hat{T}$. That is, the same state is observed at all times t separated by $2\pi/\omega_D$ (for Fig. 2 the attractor is a fixed point of $\hat{T}^6$). The smoothing of the displacement as a function of the lattice position seen in Fig. 3 is expected as ε is increased since the dispersive coupling term increases in importance. Note that in Fig. 3, x_i versus i still has two basic domains corresponding, respectively, to up and down states. Within each domain, however, there is a sinusoidal oscillation which has a wavelength of about 14 lattice sites. Based on the total lattice length of 256 points, this corresponds to a mode number of $m=\frac{256}{14}\cong 18$.

When the offset a in Eq. (5a) is varied (holding the system parameters fixed as for Fig. 3), it is found that, for different values of a, the system asymptotes to a large number of different final states, most of them fixed points of $\hat{T}$. For example, Fig. 4 is a plot of x_i versus i at $n=2048$ for $a=0.003\,01$. This initial condition again results in a fixed point final state with two domains and an $m=18$ oscillation, but the down domain has broadened considerably from that of Fig. 3. Not only does this system possess many attractors, but the actual asymptotic motion which results apparently depends sensitively on the choice of the initial condition. This final-state sensitivity[5,6] is expected in systems which possess fractal basin boundaries.[4-6]

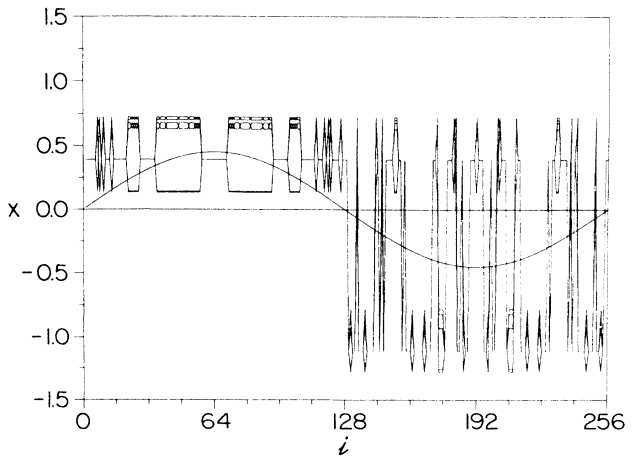

FIG. 2. Plot of the displacement x vs the chain site i for six consecutive iterates ($1025\le n\le 1031$) in the asymptotic state. Superimposed, also shown is the sinusoidal profile for the initial condition. The parameters are $\gamma=0.15$, $f=0.10$, $\omega_D=0.833$, $\varepsilon=0$, and $a=0.003$.

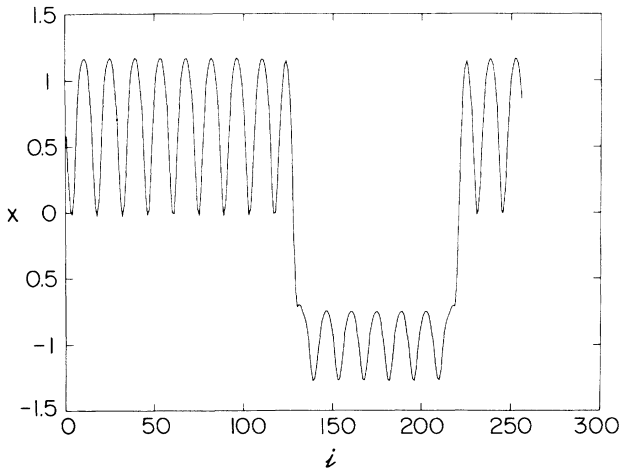

FIG. 3. Same plot as in Fig. 2 but now $\varepsilon = 1.0$, and $n = 2048$.

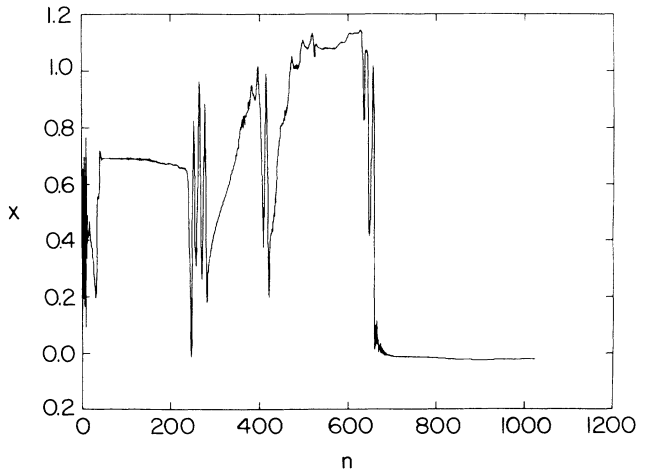

FIG. 5. Plot of displacement x vs time n for the oscillator $i = 61$ and $1 \leq n \leq 1024$. The parameters are the same as in Fig. 4.

One might expect that the sensitivity to final state described above would be reflected in the transient behavior of the chain as well. In Fig. 5 we plot the displacement of the $i = 61$ oscillator versus time between $n = 1$ and $n = 1024$ for the case of Fig. 4. Note that the time series shows intervals of roughly constant displacement interrupted by large-excursion chaotic bursts. Apparently, this oscillator tries to lock onto a fixed point, but is disrupted from doing so by disturbances originating from other portions of the lattice and is occasionally thrown in the fractal basin boundary region where it exhibits chaotic motion. At around $n = 650$, this locking-bursting behavior dies down and the oscillator settles into its final, fixed displacement state. In Fig. 6 we show a plot of x_i versus n for $i = 120$ of the same chain as in Fig. 5. This oscillator shows relatively wild chaotic behavior which also ceases at about $n = 650$. Comparing Figs. 5 and 6 between $n = 1$ and 200, we see that during the interval when oscillator 61 is almost static, oscillator 120 is experiencing relatively fast, large amplitude changes in the displacement. This is an indication that the details of the transient behavior which occurs depends on the position in the the chain.

We illustrate this with another fixed point example where $a = 0.003$ (as in Fig. 3) is used, but where the driving is slightly stronger, $f = 0.11$ instead of the value $f = 0.10$ in Fig. 3. Figure 7 shows the chain displacements as a function of lattice position superimposed from $n = 2024$ to $n = 2048$. The system again settles to a fixed point. Figure 8 is the same as Fig. 7 except that the displacements are superimposed for $600 \leq n \leq 661$. Note that the region near the left domain wall undergoes a great deal of motion while other parts of the chain, including the region near the right domain wall, is relative-

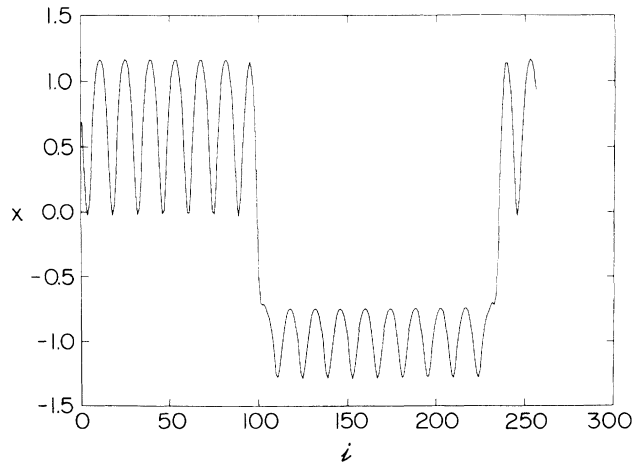

FIG. 4. Same plot as in Fig. 3 but for $a = 0.003\,01$ instead of $a = 0.003\,00$.

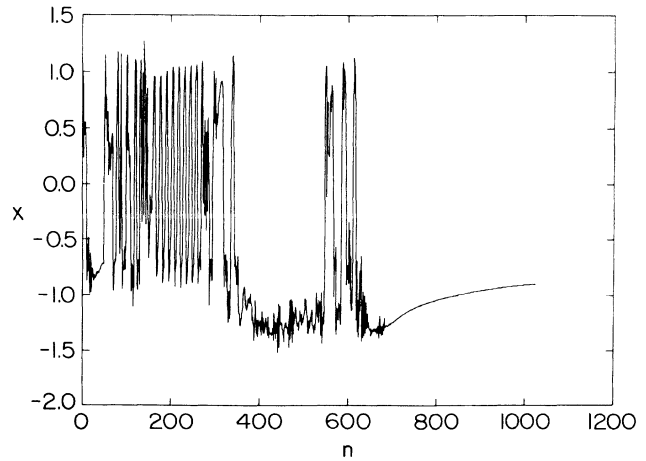

FIG. 6. Same as Fig. 5 but for the oscillator $i = 120$.

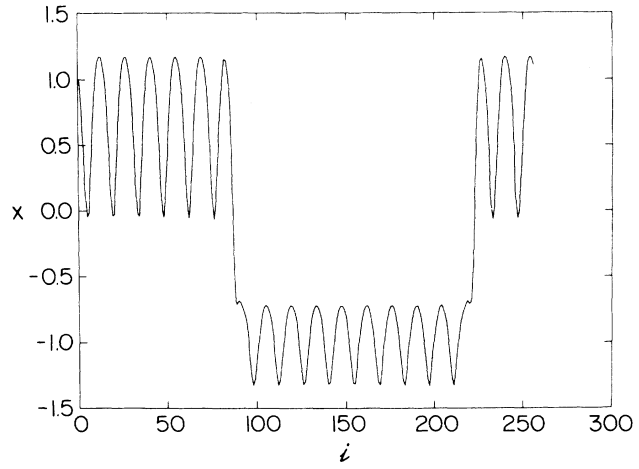

FIG. 7. Superposition of plots of x vs i for $2024 \leq n \leq 2048$. This plot is for stronger driving $f = 0.11$ with $a = 0.003$.

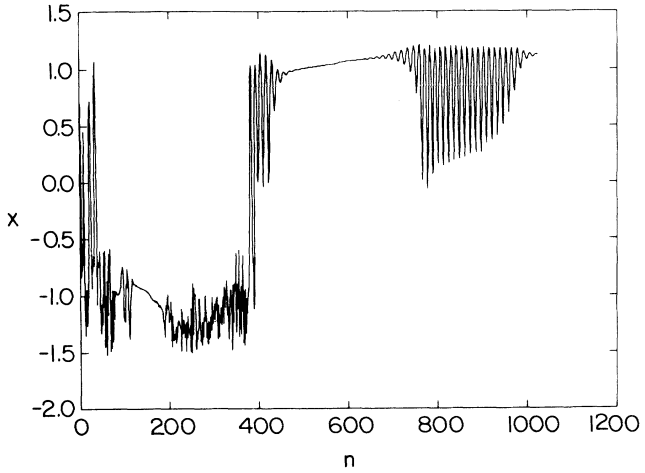

FIG. 9. Plot of x vs n for the oscillator $i = 226$ and $1 \leq n \leq 1024$. The parameters are the same as in Fig. 7.

ly static. In Fig. 9 x_i versus n is shown for $i = 226$ and $1 \leq n \leq 1024$. This oscillator is in the stable zone of Fig. 8 and undergoes relatively *static* behavior during the time interval $500 \leq n \leq 700$. This contrasts greatly with the behavior of oscillator 101, which is well in the *unstable* zone. This oscillator shows rather large excursions during the same time interval, as shown in Fig. 10. Another feature is that when Figs. 9 and 10 are compared, we see that at $n \simeq 700$ the $i = 226$ oscillator starts to undergo rapid changes just as oscillator 101 becomes roughly static. This is depicted in Fig. 11 which shows x_i versus i for $750 \leq n \leq 800$.

We speculate that the transient behavior[4] discussed in the previous examples arises from the existence of many attractors in our chain and fractal basin boundaries separating the various basins. The gross features of the spatial structure of the final state of the examples discussed so far are qualitatively similar in that there are two domains separated by sharp kinklike walls with a spatial oscillation of 14 lattice sites ($m = 18$) in each domain. The main differences between the final states are the sizes of the domains and the positions of the domain walls. We have seen that groups of nearby oscillators can lock temporarily into an $m = 18$, *transient structure* that lasts through hundreds of iterations of $\hat{T}$. Thus, it appears that the confusion experienced by an orbit as to which attractor to asymptote to shows up locally in the development of highly structured transient regions. For this model we have found that the domain walls appear to have rather complex dynamics. Standard continuous unforced models that show domain formation do not exhibit such structure. We speculate that the complex be-

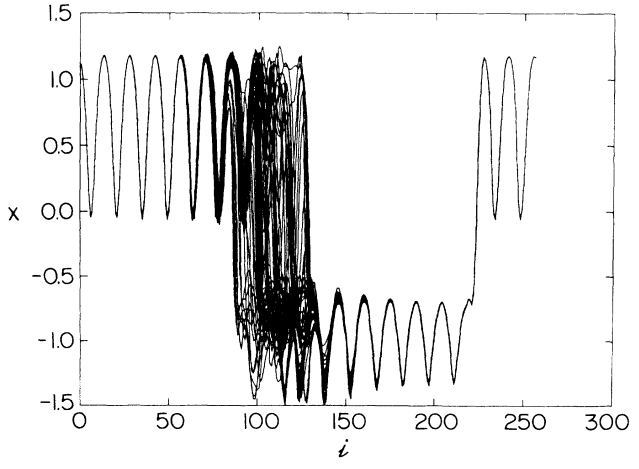

FIG. 8. Same as Fig. 7 but for $600 \leq n \leq 661$.

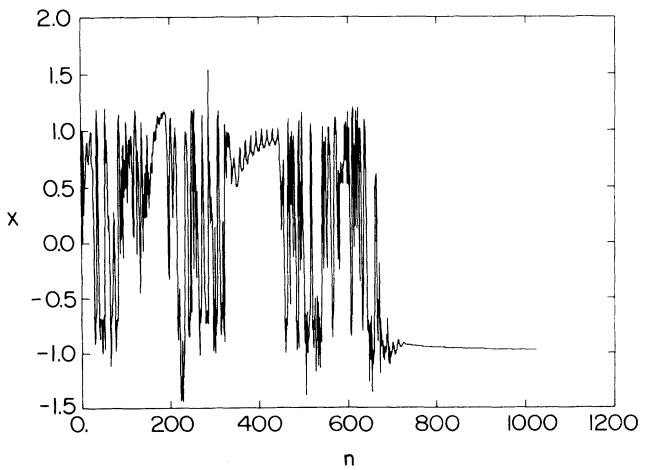

FIG. 10. Same as Fig. 9 but for the oscillator $i = 101$.

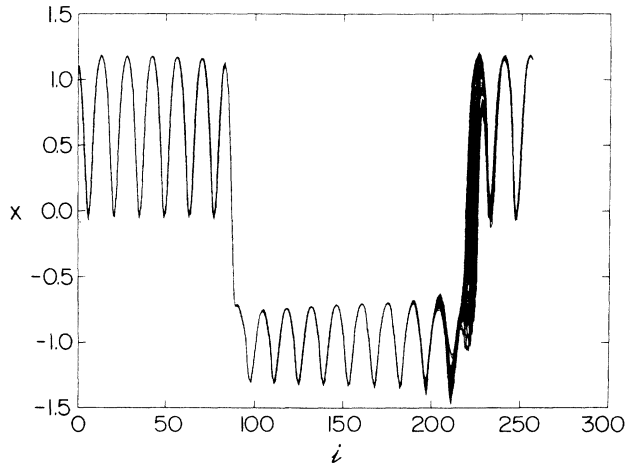

FIG. 11. Same as Fig. 7 but for $750 \leq n \leq 800$.

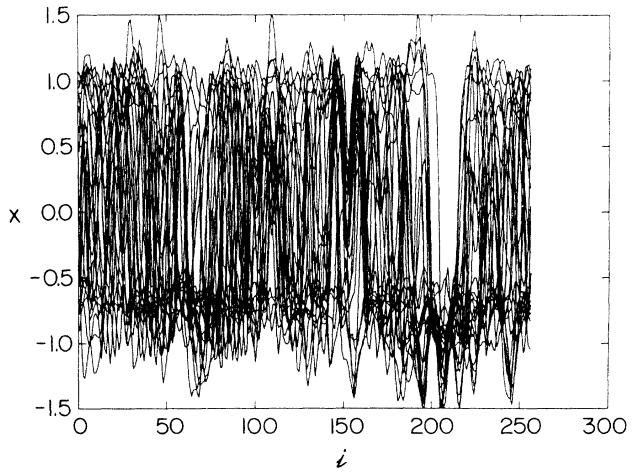

FIG. 13. Plot of x vs i showing the superposition of iterates $2024 \leq n \leq 2048$ for the same parameters as Fig. 12.

havior we observe is due to the forcing coupled with the Duffing nonlinearity rather than with the discrete-space aspect of our system.

The observation of spatio-temporal chaotic bursts during the transient phase leads us to look into the types of behavior possible when the asymptotic behavior is not as simple as fixed points. With this in mind, we examine the effects of increased driving. The local dynamics is known to make a transition to chaos around $f_c = 0.12$ when $\gamma = 0.15$, $\omega_D = 0.833$, so keeping $\varepsilon = 1.0$, we increase f.

Figure 12 shows a disordered chain state at $n = 2048$ when the driving is set to $f = f_c = 0.12$ [the initial condition is that of Eqs. (5) with $a = 0.003$]. Note the absence of the $m = 18$ structures. To get an indication of the temporal behavior of this system, Fig. 13 shows a superposition of 25 iterates of $\hat{T}$ for $2024 \leq n \leq 2048$. The time series for oscillator 1 and its power spectrum, all for the time interval $1025 \leq n \leq 2048$, are shown in Figs. 14 and 15, respectively. This behavior persists past $n = 8192$. Thus at $f = 0.12$, the chain state is highly disordered with a chaotic temporal evolution. The transition to this behavior takes place at $f \simeq 0.112$. At $f = 0.112$, the chain displacements look qualitatively the same as in Fig. 12 (see also Fig. 13), as shown in Fig. 16. However, on examination of the time series, there are similarities to what was seen in the fixed point cases, namely, that certain oscillators attempt to lock onto a local fixed point attractor and that these locking intervals are interrupted by chaotic bursts. This is seen in Fig. 17, where $x_i(n)$ is plotted for $i = 1$ from $n = 1024$ to $n = 2048$. Note the relatively stable (low-amplitude) motion from $1200 < n < 1700$. A superposition of chain displacements from $n = 1304$ to $n = 1324$ (Fig. 18) reveals the temporary formation of an orderly stable structure analogous to the $m = 18$ structure of the fixed point experiment. Oscillator 1 is in this region which accounts for its relatively small amplitude motion.

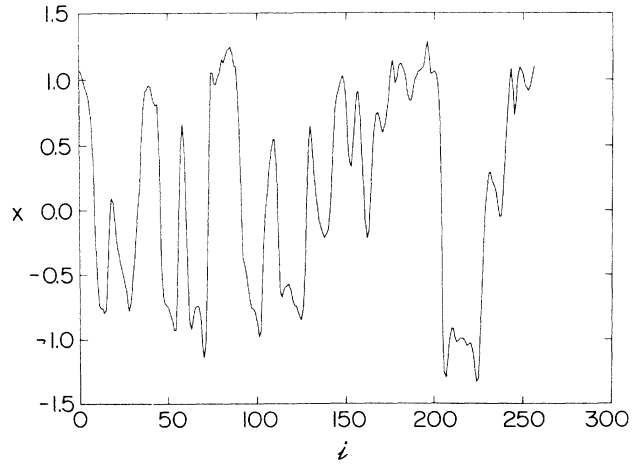

FIG. 12. The chain state x vs i for $f = 0.12$ and $n = 2048$.

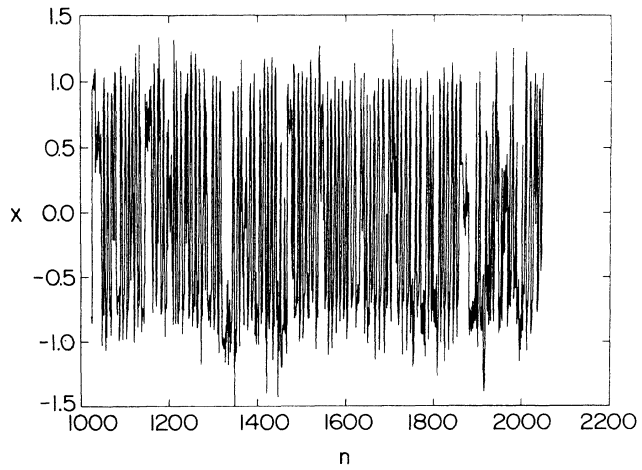

FIG. 14. Plot of x vs n for oscillator $i = 1$ and $1025 \leq n \leq 2048$ and for the same parameters as in Fig. 12.

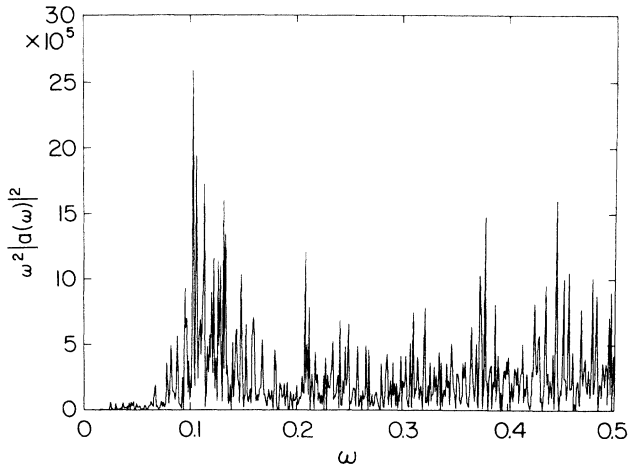

FIG. 15. Power spectrum of the trajectory shown in Fig. 14. $a(\omega)$ is the Fourier amplitude and the frequency ω is in units of ω_D.

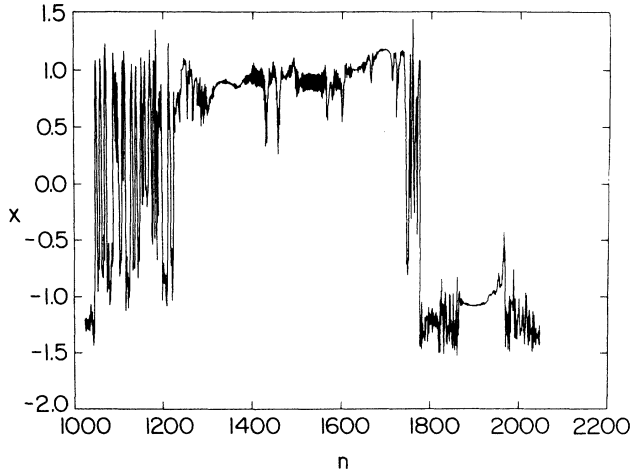

FIG. 17. Plot of x vs n for $f=0.112$, $i=1$, and $1024 \leq n \leq 2048$.

This type of transition to sustained chaos is phenomenologically similar to transitions to chaos in low-dimensional dynamical systems which undergo crises.[4] In particular, if we look at a dynamical variable as a function of time, for different values of the parameter, we observe that chaotic transients become longer and longer until we obtain sustained chaos at the crisis value of the parameter.

IV. CONCLUSION

In this paper we have numerically investigated a one-dimensional lattice system of dissipative, forced, nonlinear ordinary differential equations. The continuum limit of the this system is a nonlinear driven dissipative wave equation. In the absence of forcing, small-amplitude linear waves on the continuum system display both dispersion and damping. The parameter space of this system is very large, and so our investigation of it has not been exhaustive. The central, most interesting feature revealed in our numerical investigations was the *extreme* intermittency of the temporal behavior of the system. We believe that this is a typical feature of forced, nonlinear, spatially extended systems with wave propagation, dispersion, and damping.

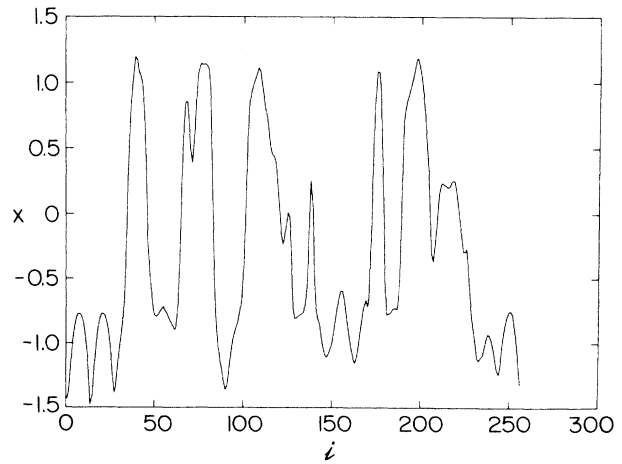

FIG. 16. Plot of x vs i for $f=0.112$ and $n=2048$.

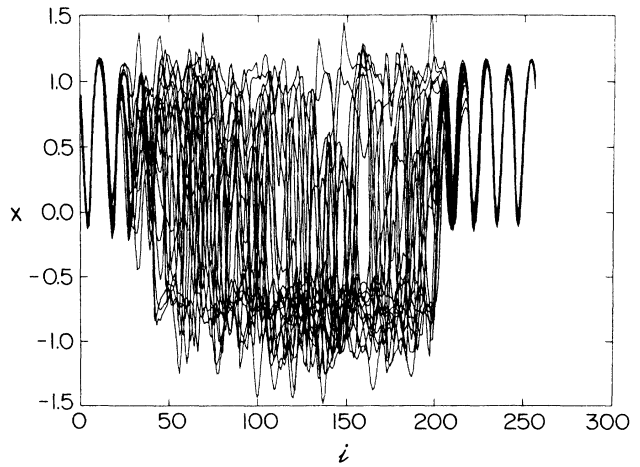

FIG. 18. Plot of x vs i for $f=0.112$ and $1304 \leq n \leq 1324$.

ACKNOWLEDGMENTS

This work was supported by the U.S. Department of Energy (Office of Basic Energy Sciences) and the Office of Naval Research (Physics). We would like to thank V. Englisch and K. Kaneko for useful discussions.

---

*Permanent address: Nordisk Atomfysik, Blegdamsvej 17, DK-2100 Copenhagen, Denmark.

†Also Department of Electrical Engineering and Department of Physics and Astronomy.

‡Permanent address: Laboratory for Laser Energetics, University of Rochester, Rochester, NY 14620.

[1]I. Waller and R. Kapral, Phys. Rev. A **30**, 2047 (1984); K. Kaneko, Progr. Theor. Phys. **72**, 480 (1984); **74**, 1033 (1985); T. Yamada and H. Fujisaka, *ibid.*, **72**, 885 (1984); Phys. Lett. **124A**, 421 (1987); R. Kapral, Phys. Rev. A **31**, 3868 (1985); H. Fujisaka and T. Yamada, Progr. Theor. Phys. **74**, 918 (1985); K. Kaneko, Physica **23D**, 436 (1986); R. Kapral and G.-L. Oppo, *ibid.* **23D**, 455 (1986); R. J. Deissler and K. Kaneko, Phys. Lett. **119A**, 397 (1987); F. Kaspar and H. G. Schuster, *ibid.* **113A**, 451 (1986); Phys. Rev. A **36**, 842 (1987).

[2]J. D. Keeler and J. D. Farmer, Physica **23D**, 415 (1988) also included longer-range coupling in their system of coupled logistic maps. There are also examples of cellular automata studies which have longer-range coupling.

[3]For example, F. C. Moon and G. -X. Li, Phys. Rev. Lett. **55**, 1439 (1985).

[4]C. Grebogi, E. Ott, and J. A. Yorke, Physica **7D**, 181 (1983).

[5]C. Grebogi, S. W. McDonald, E. Ott, and J. A. Yorke, Phys. Lett. A **99**, 415 (1983).

[6]S. W. McDonald, C. Grebogi, E. Ott, and J. A. Yorke, Physica **17D**, 125 (1985).

[7]W. H. Press, B. P. Flannery, S. A. Teukolsky, and W. T. Vetterling, *Numerical Recipes* (Cambridge University Press, New York, 1986), Chap. 15.

[8]H. Fujii and Y. Sawada, J. Chem. Phys. **69**, 3830 (1978).

[9]M. Marek and I. Stuchl, Biophys. Chem. **3**, 241 (1975).

[10]I. Stuchl and M. Marek, J. Chem. Phys. **77**, 2956 (1982).